Title

Ocean acidification increases susceptibility to sub-zero air temperatures in ecosystem engineers (*Mytilus* sp.): a limit to poleward range shifts

Authors and addresses

Jakob Thyrring[1,2*], Colin D. MacLeod[1,3], Katie E. Marshall[1], Jessica Kennedy[1], Réjean Tremblay[4] & Christopher D. G. Harley[1,5]

[1]Department of Zoology, University of British Columbia, V6T 1Z4, Vancouver, British Columbia, Canada
[2]Department of Ecoscience – Marine Ecology & Arctic Research Centre, Aarhus University, 8000, Aarhus C, Denmark
[3]Department of Biological Sciences, University of Alberta, T6G 2E9, Edmonton, Alberta, Canada
[4]Institut des sciences de la mer, Université du Québec à Rimouski, G5L 3A1, Rimouski, Quebec, Canada
[5]Institute for the Oceans and Fisheries, University of British Columbia, V6T 1Z4, Vancouver, British Columbia, Canada

*Corresponding author: thyrring@ecos.au.dk

ORCID
Jakob Thyrring – 0000-0002-1029-3105
Colin MacLeod – 0000-0002-5963-3713
Katie Marshall – 0000-0002-6991-4957
Jessica Kennedy - 0000-0002-7979-1516
Réjean Tremblay – 0000-0003-2590-8915
Christopher D.G. Harley – 0000-0003-4099-943X

Keywords
Blue mussel; Intertidal; Fatty acids; $LLT_{50;}$ Multiple stressors; Thermal tolerance

Abstract

Ongoing climate change has caused rapidly increasing temperatures, and an unprecedented decline in seawater pH, known as ocean acidification. Increasing temperatures are redistributing species towards higher and cooler latitudes which are most affected by ocean acidification. Whilst the persistence of intertidal species in cold environments is related to their capacity to resist sub-zero air temperatures, studies have never considered the interacting impacts of ocean acidification and freeze stress on species survival and distribution. A full-factorial experiment was used to study whether ocean acidification increases mortality in *Mytilus* spp. following sub-zero air temperature exposure. We examined physiological processes behind variation in freeze tolerance using ^{1}H NMR metabolomics, analyses of fatty acids, and amino acid composition. We show that low pH conditions (pH = 7.5) significantly decrease freeze tolerance in both intertidal and subtidal populations of *Mytilus* spp. Under current day pH conditions (pH = 7.9), intertidal *M. trossulus* were more freeze tolerant than subtidal *M. trossulus* and *M. galloprovincialis*. Opposite, under low pH conditions, subtidal *M. trossulus* was more freeze tolerant than the other groups. We observed a marked shift from negative to positive metabolite-metabolite correlations across species under low pH conditions, but there was no evidence that the concentration of individual metabolites or amino acids affected freeze tolerance. Finally, pH-induced changes in the composition of cell membrane phospholipid fatty acids had no effect on survival. These results suggest that ocean acidification can offset the poleward expanding facilitated by warming, and that reduced freeze tolerance could result in a niche squeeze if temperatures become lethal at the equatorward edge.

1. Introduction

The rapid rise in atmospheric CO_2 concentration since the industrial revolution has increased global air and water temperatures and caused ocean pH to decline (a process termed ocean acidification [OA]) at rates unprecedented in the geological history (Hönisch et al., 2012). These environmental changes are causing species range shifts and cascading ecological effects across the globe, resulting in regime shifts and altered food web structures (Kortsch et al., 2012; Wernberg et al., 2016). For example, the fish assemblage around the Svalbard archipelago, located in the Arctic Ocean (78°N), is borealizing as Arctic species have retracted northwards to cooler areas while boreal species have become dominant (Fossheim et al., 2015). Co-occurring OA is, furthermore, predicted to have severe consequences for marine organisms and communities, and a large body of research has shown a wide range of negative effects. Decreased pH weakens shell production (MacLeod and Poulin, 2015) and increases dissolution in calcifying organisms, which are therefore generally more vulnerable to OA compared to other organisms (Kroeker et al., 2010). Ocean acidification has also been found to increase heart rates in some invertebrate species (Lim and Harley, 2018) and alter benthic community structure (Brown et al., 2018). Elevated temperatures and OA have furthermore been observed to interact in various ways, causing heterogenic physiological responses across species, depending on taxon and life-stage (Harvey et al., 2013). Indeed, these two stressors may disproportionally alter species interactions and biodiversity in marine ecosystems (Franzova et al., 2019; Nagelkerken and Munday, 2016).

While the vast majority of OA and climate change research has focused on lower latitude systems, studies have rarely considered the impacts on species at their poleward edge. The poleward edge of subtidal ectotherms is determined by low water temperatures (Sunday et al., 2012), however the distribution of intertidal species is also controlled by their capacity to tolerate sub-zero air temperatures during emersion (Kennedy et al., 2020; Reid and Harley, 2021; Thyrring et al., 2019).

On rocky shores, canopy-forming macroalgae shelter the understory communities from extreme sub-zero air temperatures (Sejr et al., 2021), and where cold enough, an ice foot forms on the rocky surface, creating a warmer protective microhabitat increasing survivorship of intertidal organisms residing below (Scrosati and Eckersley, 2007; Thyrring et al., 2017a). However, as temperatures increase at the northern range edge where ice forms, organisms face sub-zero air temperatures when emerged at low tides as the ice foot melts, offsetting the otherwise facilitative effect of ocean warming on range expansions.

To survive sub-zero air temperature exposure, ectothermic animals depend on various freeze tolerance mechanisms (Storey and Storey, 1996; Toxopeus and Sinclair, 2018), yet despite the principle importance of freeze tolerance in sessile intertidal species, the underlying physiological processes remain poorly understood (Kennedy et al., 2020). Suggested mechanisms behind freeze mortality are excessive osmotic stress and structural damage to cell membranes, as ice forms in the extracellular water, dehydrating the cell and destabilizing the membrane (Meryman, 1971; Storey and Storey, 1988). To avoid cell dehydration, some species accumulate cryoprotectants, such as metabolites (low molecular weight cryoprotectants), to protect against intracellular osmotic stress as water is lost to the extracellular space. In intertidal bivalves, metabolites and anaerobic byproducts such as trimethylamine n-oxide (TMAO), betaine, taurine and strombine, likely to act as cryoprotectants, increasing freeze tolerance (Kennedy et al., 2020; Loomis et al., 1988). While under-explored, it also appears that many intertidal species may have an array of ice binding proteins that help manage ice growth and propagation (Box et al., 2022).

Freeze tolerance in some ectotherms is also associated with the composition of the cell membrane phospholipid fatty acids, which are sensitive to temperature variation (Hazel, 1995). Functional membranes must exist in a fluid liquid-crystalline phase maintained by the composition of the phospholipids. Low temperatures decrease membrane fluidity, and the membrane becomes partly

dysfunctional, losing selective properties and leaking cell contents (Hazel 1995). Ectotherms can counteract this effect by desaturating the membrane (increasing the proportion of unsaturated phospholipids) and adjusting cholesterol levels. This mechanism, termed homeoviscous adaptation, has been shown in a wide range of marine and terrestrial animals (Storey and Storey, 1988), and intertidal bivalves can remodel phospholipids in response to temperature changes (Pernet et al., 2007; Thyrring et al., 2017c; Williams and Somero, 1996). Despite this progress on the mechanisms of cold and freeze tolerance in intertidal species, it is completely unknown whether OA interacts with these. High latitude cold water is able to absorb significantly more CO_2 than lower latitude warmer water, and therefore seawater pH is decreasing most rapidly at these latitudes (Fassbender et al., 2017). Ocean acidification decreases pH in osmoconformers with a low capacity to regulate internal pH levels (e.g., bivalves), which could lead to disruption of cellular processes, and shifts in osmotic balance (Wittmann and Pörtner, 2013; Zhao et al., 2020). Thus, OA may decrease freeze tolerance and increase animal vulnerability to sub-zero air temperature exposure, yet the interaction between OA and freeze tolerance interactions remains to be explored.

Bivalves of the genus *Mytilus* are distributed in intertidal habitats in both the Northern and Southern Hemisphere (Hilbish et al., 2000; Mathiesen et al., 2017). *Mytilus* sp. are commercially, and ecologically important ecosystem engineers creating habitats for a diverse associated fauna and are widely used as model organisms for studying impacts of various stressors (Barrett et al., 2022; Telesca et al., 2019; Thyrring et al., 2015). *Mytilus* sp. can survive tissue freezing, and are expanding at higher latitudes in response to global warming (Thyrring et al., 2017a), however, the performance and survival of *Mytilus* sp. at their poleward edge remain poorly understood.

The focus of this study is two *Mytilus* spp. found in British Columbia, Canada; the invasive Mediterranean mussel *M. galloprovincialis,* and the native bay mussel *M. trossulus*, allowing a comparison of responses among native and invasive species. By investigating the effects of OA on

freeze tolerance in these species, we test the hypothesis that OA will generally increase mortality in intertidal species living near their poleward range edge due to an increased susceptibility to sub-zero air temperatures during emersion. Mussels from both the intertidal and subtidal realm were investigated to detect whether previous exposure to air has any effects on freeze tolerance. Specifically, we predict that (1) intertidal animals are more freeze tolerant than subtidal conspecifics, (2) native *M. trossulus* is more freeze tolerant than *M. galloprovincialis,* and (3) OA will increase freeze mortality in both species. Finally, we hypothesize that mechanistic processes including (I) a destabilized cell membrane caused by variation in the unsaturation state of membrane phospholipids, (II) and variation in the composition and concentration of selected molecular cryoprotectants will explain variation in freeze tolerance.

2. Materials and Methods

2.1 Animal collection and holding conditions

Three categories of *Mytilus* mussels were collected on 8–10 December 2019 in the strait of Georgia, British Columbia, Canada; 1) subtidal *M. galloprovincialis* obtained from an aquaculture farm at Saltspring Island, 2) subtidal *M. trossulus* collected from floating docks at the Jericho Royal Vancouver Yacht Club in the Burrard Inlet, and 3) intertidal *M. trossulus* collected at low tide from Tower Beach in the Burrard Inlet (Collection permit number XMCFR 7 2019; Fisheries and Oceans Canada). Intertidal *M. galloprovincialis* was not considered as no intertidal populations are established in region. All mussels were kept for a 72-hour adjustment period in aerated aquaria of similar environmental conditions as the collection site measured on the days of collection (7°C, pH = 7.9, and salinity 20.5). No mussels died during the adjustment period.

Prior to sub-zero air temperature exposure, mussels were maintained in low (7.50 pH) or control (7.90 pH) conditions for 10 days using three incubators (Panasonic MIR 154, Panasonic, Japan) for low pH

158 conditions and three for control conditions (no mussels died during the 10 days). Each incubator was
159 set to 7°C and contained three 5L glass aquarium that held three envelopes of 0.5cm gauge, rigid
160 plastic mesh (25×24cm) that separated the three categories of mussel but allowed easy flow through
161 of seawater (salinity 20-21). Each envelope was marked with a different colored zip tie to indicate
162 which category of mussel it contained.
163
164 *2.2 Seawater manipulation*
165 The two selected pH conditions covered a realistic range of pH values currently observed or predicted
166 for the Southern Strait of Georgia; a control (pH = 7.9) and a low pH treatment (pH = 7.5) (Ianson et
167 al., 2016). The low pH treatment was established by using two Smart-Trak® mass flow controllers
168 (Sierra Instruments, Inc., CA, USA) to mix 100% CO_2 (PraxAir Canada Inc., CB, Canada) and CO_2-
169 free air, which was then bubbled into three acidified seawater aquaria to achieve target values of 7.50
170 pH. CO_2-free air was generated by using a small compressor to pump ambient air through a 500 mL
171 Nalgene canister that contained Soda Lime (Ormond Veterinary Supply Ltd., ON, Canada). A flow
172 rate of 3.3 cm^3/s of 100% CO_2 gas and 4.11 L/min of CO_2-free air was used to reach the target pH.
173 Our system also removed moisture from ambient air to protect the mass flow controllers from water
174 damage. This was achieved by running the ambient-air gas lines through a small refrigerator to reduce
175 air temperature and cause water to precipitate into a water trap, and by installing a second 500 mL
176 Nalgene containing desiccant (WA Hammond Drierite, OH, USA) in series with the soda lime
177 container. Control conditions (7.90 pH) were maintained by mixing ambient air and CO_2-free air. The
178 use of CO_2-free air was necessary as ambient air was artificially high in CO_2 due to poor ventilation
179 in the lab. As with the low pH treatment, ambient air was pumped through a Soda Lime-filled 500
180 mL Nalgene canister using a small compressor before being connected to a three-way splitter and
181 bubbled into seawater aquaria, while ambient air was bubbled into the control aquaria using a second

set of tubes connected to low power aquarium air pumps (Fusion 700 Air Pump). Air flow from the small aquarium pumps was fine-tuned by placing an adjustable clamp on the flexible tubing which connected pump and air stone to increase or decrease the flow of CO_2 enriched ambient air to achieve 7.90 pH. Carbon dioxide in ambient "lab" air was monitored constantly using a Qubit S151 CO2 gas analyzer (Qubit Systems, ON, Canada), which showed that CO_2 fluctuated during the day between 400 ppm and 600 ppm CO_2 reaching the maximum during the day while people were working in the lab. Consequently, the input of ambient air into control tanks was monitored and adjusted daily (mainly during the day) to maintain target pH values. Prior to adjusting seawater pH, we mixed filtered seawater (provided by the Vancouver Aquarium and transported by the City of Vancouver) with de-chlorinated distilled fresh water to create a 20-21 ppt solution which was the salinity recorded at the collection sites. Mussels were able to feed on phytoplankton naturally occurring in the water, and we replaced 50% of the seawater from each tank daily to prevent the buildup of faeces and maintain uniform seawater chemistry parameters.

2.3 Carbonate chemistry

Seawater pH was measured daily in all aquaria using a hand-held pH meter (Table 1 - Oakton pH 450 (±0.01 pH), Oakton Instruments, IL, USA) calibrated with two saltwater buffers, as described in (MacLeod et al., 2015) to provide pH measurements on the Total Hydrogen Ion Scale (pH_T). To further characterize the seawater carbonate chemistry, seawater samples (300 mL) were collected from one randomly selected aquarium in each incubator at the start and end of the experiment. These samples were fixed with a saturated solution of mercuric chloride (RICCA Chemical Company, TX, USA) and analyzed using the "burke-o-lator" at Hakai Institute (Quadra Island, BC, Canada) (for details of this system see (Evans et al., 2019)). This analysis generated values for DIC and pCO_2 which were then used in combination with temperature and salinity data to calculate all relevant

carbonate parameters (Supplementary Table S1) using the MATLAB version of CO2SYS (van Heuven et al., 2011).

2.4 Sub-zero temperature exposure

After 10 days, mussels were exposed to seven sub-zero air temperatures (-5, -6, -7, -8, -9, -12, -15 °C) for two hours by placing animals in individual plastic tubes inserted in wells drilled into a precooled aluminum block cooled by refrigerated circulation baths (Thermo Fisher Scientific Inc., MA, USA). Fifteen mussels (mean shell length 37.69 mm ± 3.14 s.d.) from each mussel category (subtidal *M. galloprovincialis* and *M. trossulus*, and intertidal *M. trossulus*) and pH condition (pH =7.9 and pH = 7.5) were used at every temperature for a total of 720 mussels. Individual body temperatures were recorded at 0.5 s intervals using Type-T thermocouples (Omega, QC, Canada) placed next to the shell inside the plastic tube and connected to TC-08 thermocouples interfaces (Pico Technology, United Kingdom) that interfaced to a computer running PICOLOG software (Picotech, United Kingdom), which continuously monitored body temperatures. Continuously body temperature monitoring allowed us to determine any exothermic release of heat owing to ice formation. The lowest temperature prior to this event is termed the supercooling point (SCP), and the SCP indicates that internal ice formation occurred. After two hours of sub-zero air exposure, all mussels were transferred back to their respective pre-freezing pH condition aquaria for recovery where they were monitored daily for five days to record mortality. Mortality was checked daily with mussels considered dead if they did not close their shells when touched. Dead mussels were immediately removed from the aquaria, and had their shell length measured to nearest mm.

2.5 Amino acid analysis

Total amino acid analysis was performed on gill tissue from mussels collected after 10 days of pH exposure (mean dry weight = 15.46 mg ±0.61 s.d., n = 5) at the Proteomics, Analytics, Robotics & Chemical Biology Centre (SPARC - https://lab.research.sickkids.ca/sparc-molecular-analysis/services/amino-acid-analysis/), Hospital for Sick Children, Toronto, ON, Canada, using the Water Pico-Tag System (Water Corporation, WA, USA). The final concentration of each amino acid was calculated in $\mu g \cdot mg^{-1}$ and then expressed as relative concentration (% of total amino acids). It should be noted that this amino acid analysis did not allow discrimination between Asn/Asp and Gln/Glu.

2.6 Fatty acid analysis

Fatty acid (FA) analyses were performed on gills (collected after 10 days of pH exposure), a tissue exposed directly to temperature changes (mean wet weight = 0.38g ±0.1 s.d., n = 5). Total lipids were extracted by grinding in a dichloromethane: methanol (2:1, v/v) solution following a slightly modified Folch procedure (Parrish, 1999). Lipid extracts were separated into neutral and polar fractions by column chromatography on silica gel micro-columns (30 × 5 mm i.d., packed with Kieselgel 60, 70−230 mesh; Merck, Germany) using chloroform: methanol (98:2, v/v) to elute neutral lipids, followed by methanol to elute polar lipids (Marty et al., 1992). Fatty acid profiles were determined on fatty acid methyl esters (FAMEs) using sulphuric acid:methanol (2:98, v/v) and toluene. FAMEs of neutral and polar fractions were concentrated in hexane, and the neutral fraction was purified on an activated silica gel with 1 ml of hexane:ethyl acetate (1:1 v/v) to eliminate free sterols. FAMEs were analyzed in the full scan mode (ionic range: 60−650 m/z) on a Polaris Q ion trap coupled multi-channel gas chromatograph 'Trace GC ultra '(Thermo Scientific, USA) equipped with an auto sampler model Triplus, a PTV injector and a mass detector model ITQ900 (Thermo

Scientific, USA). The separation was performed with an Omegawax 250 (Supelco) capillary column with high-purity helium as a carrier gas. Data were treated using Xcalibur v.2.1 software (Thermo Scientific, USA). Methyl nondecanoate (19:0) was used as an internal standard. FAMEs were identified and quantified using known standards (Supelco 37 Component FAME Mix and menhaden oil; Supleco) and were further confirmed by mass spectrometry (Xcalibur v.2.1 software).

2.7 ^{1}H NMR analysis

One-dimensional, 600 MHz proton nuclear magnetic resonance spectroscopy (^{1}H NMR) was used to measure the metabolite profiles of gill tissue (collected after 10 days of pH exposure). ^{1}H NMR is ideal for measuring low molecular weight, polar metabolites such as osmolytes and anaerobic byproducts. Sample preparation was based on (Cappello et al., 2013). A 100 mg sample of gill tissue was excised (n = 5), dried with a Kimwipe to remove excess water and frozen at −80°C. Frozen tissue was homogenized in 400 µl cold methanol and 85 µl cold water-xylitol solution (5 mM xylitol as an internal control) using a bead homogenizer (Bullet Blender 50 Gold Model: BBX24, Next Advance) with approximately 200 µl of 3.2 mm round stainless steel beads, for 10 min at setting 8 in 1.5 ml microcentrifuge vials. After adding 400 µl chloroform and 200 µl water to the samples, they were vortexed for 60 s, left on ice for 10 min for phase separation, and centrifuged for 5 min at 2000 rpm. The upper methanol layer (600 µl) containing the polar metabolites was transferred into new vials, dried in a centrifugal vacuum concentrator (Eppendorf 5301), and then stored at −80°C. Immediately prior to ^{1}H NMR analysis, the dried polar extracts were resuspended in 600 µl of 0.1 mol/l sodium phosphate buffer (pH 7.0, 50% deuterium oxide, Sigma-Aldrich) containing 1 mmol/l 2,2-dimethyl-2-sila-pentane-5-sulfonate (DSS; Sigma-Aldrich) as internal reference. The mixture was vortexed for 60 s and transferred to a 5 mm NMR tube.

^{1}H NMR spectra were acquired using Bruker Avance 600 with cryoprobe and Bruker Avance III 600 spectrometers. TopSpin software version 2.1 (Bruker) was used to process spectra collected with the Bruker Avance 600 spectrometer with cryoprobe, and TopSpin version 3.5 (Bruker) was used with the Bruker Avance III 600 spectrometer. Experiments required 15 minutes of acquisition time and were performed at room temperature.

Peak identification of the NMR spectra was performed with Chenomx NMR Suite 9.0 (Chenomx, AB, Canada) that uses the Human Metabolome Database compound spectral reference library (Wishart et al., 2018). First, line broadening of 2.5 Hz, automatic phase correction, and manual baseline correction were performed with Chenomx Processor (within the Chenomx NMR Suite software). Then, determination of metabolite concentrations was performed using Chenomx Profiler, which determines the concentrations of individual metabolites using the concentration of a known DSS signal. Metabolite concentrations are reported as mmol/100 mg gill wet mass.

2.8 Statistical analysis

2.8.1 Survival

Statistical analyses were performed using the R software (R version 3.5.2). A logistic regression model was used to calculate LLT_{50} values (the lower lethal temperature where 50% of the population survived). A binomial generalized linear model (GLM) with a logit link function, was used to determine the effects of air temperature and pH treatment on survival within each mussel category, and the difference in LLT_{50} were estimated using 95% confidence intervals (CI) with non-overlapping CI indicating a significant difference (Deere et al., 2006). Differences in the supercooling point (SCP) among mussel categories and pH treatment was analyzed using a two-way ANOVA. Final models were validated by plotting residuals versus fitted values, versus each covariate in the model (Zuur and Ieno, 2016).

301 *2.8.2 Metabolomics and fatty acids*

302 Generalized linear models and ANOVAs were used to determine which metabolites and fatty acids
303 differed significantly after low pH exposure. Pearson's correlations were furthermore used to detect
304 alternations in metabolite-metabolite associations following low pH conditions (Jahagirdar and
305 Saccenti, 2020), and relationships were visualized using heat maps. The fatty acids explaining most
306 of the dissimilarity between mussel categories and pH treatments were identified using a SIMPER
307 analysis (See the full list of FA founds in Supplementary Table S2). This analysis revealed that 13
308 fatty acids explained ~90% of the Bray–Curtis dissimilarity amongst fatty acid profiles between the
309 control and low pH environment (Table 2). We therefore focused all subsequent fatty acid analyses
310 on these 13 fatty acids. Principle component analysis (PCA) was used to the interpretation of
311 differences in the metabolomic composition among mussel categories. ANOVAs were used to
312 evaluate differences in the concentrations of amino acids, and GLMs to evaluate the distribution of
313 saturated fatty acids (SFA), monounsaturated fatty acids (MUFAs), polyunsaturated fatty acids
314 (PUFAs), and the unsaturation index (UI), which is an index for the number of double bonds per 100
315 molecules of fatty acids, among the three mussel categories and pH Treatment. Post-hoc pair-wise
316 tests were used to compare significant treatment effects ($P < 0.05$). Detailed data exploration was
317 carried out prior to any analysis (Zuur et al., 2010). Once valid models were identified, we re-
318 examined the residuals to ensure all model assumptions were acceptable.
319
320 **3. Results**
321 *3.1 Survival*
322 Validation of ANOVAs and GLM models indicated no violation of model assumptions. There were
323 no significant effects of pH conditions (ANOVA; $p > 0.05$) or mussel categories (ANOVA; $p > 0.05$

on the SCP, and freezing of the tissue was observed in all mussels exposed to temperatures below -7°C.

We investigated the effect of pH and sub-zero air temperature on survival using GLMs. There were no significant interactions between the effect of pH and air temperature on any mussel category, and the interaction term was excluded in the final GLM models. Lower sub-zero air temperature significantly decreased the survival of mussel in all three categories exposed to both control and low pH conditions (Fig. 1; Supplementary Table S3). Under control conditions (pH = 7.9), the lower lethal temperature at which 50% of the population perish (LLT_{50}) was significantly lower in intertidal *M. trossulus* (−10.56 °C ± 0.80 CI) compared to subtidal *M. trossulus* (-9.12°C ± 0.48 CI) and subtidal *M. galloprovincialis* (-7.62 °C ± 0.49 CI), which was the least freeze tolerant species (Fig. 1). Following exposure to low pH (pH = 7.5), survival significantly decreased after sub-zero air exposure in all three mussel categories (Fig. 1; Supplementary Table S3). Accordingly, the LLT_{50} of intertidal *M. trossulus* was -7.53°C ± 0.26 CI, while the LLT_{50} was -8.04°C ± 0.32 CI and -6.69°C ± 0.17 CI for subtidal *M. trossulus* and subtidal *M. galloprovincialis*, respectively. Thus, subtidal *M. trossulus* was the most freeze tolerant category under low pH conditions. It should be noted that only one *M. galloprovincialis* (6.66%) survived exposure to -8°C.

3.2 Metabolomics and fatty acids

We compared the composition of metabolites using PCA plots, which showed that the three mussels categories clustered together, suggesting no differentiation in their metabolic profiles (Supplementary Fig. S1). The predominate osmolytes were alanine, aspartate, betaine, glycine, malonate, taurine, trimethylamine and trimethylamine n-oxide (TMAO) (see Supplementary Table S4 for full list of all metabolites obtained from the ^{1}H NMR analysis), but we detected no significant changes in their concentration among the two pH treatments or mussel categories (Fig. 2). Likewise, were there no

348 significant differences in the concentration of any amino acids among mussel categories or pH
349 treatment (Table 3). A metabolite-metabolite Pearson correlation analysis of the predominate
350 osmolytes revealed that each mussel category had a unique metabolite-metabolite relationship under
351 control pH conditions (Fig. 3 Upper panel). Low pH conditions changed the metabolite-metabolite
352 relationship in all three mussel categories (Fig. 3 Lower panel); A marked shift from negative to
353 positive correlations was observed across all metabolites in *M. trossulus* where the number of positive
354 correlations increased by circa 53% in intertidal *M. trossulus* and 109% in subtidal *M. trossulus*. In
355 *M. galloprovincialis*, the number of positive metabolite-metabolite correlations decreased from 11 to
356 10 (Fig. 3).
357 Thirteen fatty acids contributed ~90% of the difference in membrane composition between the
358 control and low pH treatment mussels (Table 2). While the fatty acid profiles in intertidal *M. trossulus*
359 were unaffected by low pH exposure (Table 2; Fig. 4), the low pH treatment caused an increase in
360 the amount of SFA and a decrease of PUFA in subtidal *M. galloprovincialis* and *M. trossulus* (Fig.
361 4), which resulted in a significant decrease in the degree of unsaturation (GLMs; $p < 0.05$; Table 2;
362 Fig. 4). Accordingly, the unsaturation index (UI) was significantly higher in intertidal than subtidal
363 *M. trossulus* after pH exposure (TukeyHSD, $p = 0.0002$).

364
365
366 *3.3 Seawater chemistry*

367 Mean pH measurements from the hand-held pH meter showed relatively good agreement with our
368 target acidified treatment (7.5 $pH_T \pm 0.03$-0.06 s.d.), although there was a greater degree of variability
369 in the control treatments (7.9 $pH_T \pm 0.12$-0.19 s.d.) due to fluctuating ambient pCO_2 (Table 1;
370 Supplementary Fig. S2). There was also some disagreement between our measured pH_T and pH
371 calculated using DIC and pCO_2 data (Supplementary Table S5). The discrepancies in our control
372 treatments were the result of the highly variable ambient pCO_2 and the corresponding adjustments

373 we frequently made to our gas delivery system. On average, these fluctuations did not cause
374 significant deviations from our target pH values, as shown by our hand-held pH_T data (Table 1), but
375 were more pronounced in the data taken from discrete, single time-point water samples. In all but one
376 instance, the difference between directly measured and calculated pH for a single time point, i.e. the
377 direct pH_T measurement made at the time the discrete water sample was taken, was within the
378 standard deviation of mean pH measurements taken over the two-week period. The regulation of OA
379 simulation systems with potentiometric pH meters has been shown to be reliable (MacLeod et al.,
380 2015), and therefore it is likely that the discrepancy between discrete and hand-held pH_T data was not
381 indicative of substantial deviations in seawater chemistry target values.
382 The addition of CO_2 free air to the controls also resulted in lower-than-expected pCO_2 values in both
383 start and end point data from those treatments (Supplementary Table S1 and S5). We also observed
384 some anomalous values for end point total alkalinity and DIC in our control treatment which were
385 attributed to shell calcification and insufficient water replacement rates (Supplementary Table S1 and
386 S5). These values were not indicative of the seawater chemistry parameters over the entire
387 experimental period, as described above, but are included for completeness.
388
389 *3.4 Seawater chemistry variability*
390 In contrast to open oceans where pH is stable (Hofmann et al., 2011), daily and seasonal fluctuations
391 can exceed 0.7 pH units in coastal ecosystems (Baumann et al., 2015; Hofmann et al., 2011;
392 Menéndez et al., 2001; Santos et al., 2011; Semesi et al., 2009), where dense blue mussel beds have
393 been found in areas characterized by $\Omega_{arag} < 0.5$ (Duarte et al., 2020). Specifically, along the intertidal
394 rocky shoreline of the Northwest Pacific, where mussels for this study was collected, pH values
395 naturally decline below 7.6 (Ianson et al., 2016; Kroeker et al., 2016). Thus, while pH conditions in
396 our aquariums fluctuated (control 7.84±0.19–7.92±0.12 | acidified 7.49±0.05–7.55±0.03), the

397 variability was within the range of *in situ* fluctuation rates. Our control conditions therefore represent
398 actual *in situ* conditions, and the final average difference in pH between the control (7.88) and
399 acidified (7.52) represented our target values (7.9 pH and 7.5 pH). The natural variation in coastal
400 pH also challenges the common belief that Ω_{arag} should be >1 (non-corrosive conditions) to represent
401 control conditions in OA experiments. Instead, we argue that control conditions should reflect actual
402 pH levels on the site of collections, regardless of the Ω_{arag} level. While we acknowledge that our
403 regulation of seawater chemistry could be improved, we believe that changes in mussel survival were
404 caused by changes in average pH, rather than variation in pH or other parameters. Our rationale is
405 supported by the fact that intertidal mussels exhibited the largest decrease in survival upon exposure
406 to reduced pH plus freezing, and as they are typically exposed to much greater variability in seawater
407 chemistry and temperature than subtidal mussel populations, it is highly unlikely that variability had
408 the most pronounced and negative affect on this group.
409
410 **Discussion**
411 Climate change is redistributing species towards cooler environments but understanding how
412 different drivers interact to shape species distribution ranges is essential for predicting patterns and
413 rates of change. At higher latitudes, expanding species face a suite of novel abiotic conditions
414 including low temperatures, and a decreasing seawater pH (Fassbender et al., 2017). The goals of this
415 study were to investigate the combined effect of low seawater pH and sub-zero air temperature stress
416 on survival of two *Mytilus* spp. and compare the responses between a native and invasive congener.
417 Intertidal individuals of the native bay mussel *M. trossulus* were significantly more freeze tolerant
418 than subtidal *M. trossulus* individuals which were in turn more freeze tolerant than the invasive
419 Mediterranean mussel *M. galloprovincialis*. Following exposure to acidified seawater, our data
420 demonstrated a significant negative effect on freeze tolerance and survival across all species-habitat

421 combinations. Interestingly, the intertidal population of *M. trossulus* was most impacted by
422 acidification, while subtidal *M. trossulus* was the least affected, becoming most freeze tolerant.
423 Cellular accumulation of metabolites and reconfiguration of membrane fatty acids were uncorrelated
424 with the observed variation in survival among mussel categories under both control and acidified
425 conditions, which could be related to short term exposure. The homeoviscous adaptation related to
426 the inverse relationship between the unsaturation index (UI) and acclimation temperature was mainly
427 related to 22:6ω3 and 20:5ω3 levels (Pernet et al., 2007), thus the more than two time lower content
428 of 22:6ω3 and 20:5ω3 in subtidal *M. trossulus* in low pH condition, could suggest that long term
429 exposure to low pH decrease the cold acclimation capacity for this group of mussels. Although, we
430 were unable to explain the observed variation in survival, we show that exposure to acidified water
431 changed metabolite-metabolite associations in all three mussel categories, indicating that
432 perturbations in seawater chemistry induce molecular alterations in these species.
433 Under present-day conditions (our control pH treatment), both the intertidal and subtidal *M. trossulus*
434 category of the native *M. trossulus* were more freeze tolerant than the invasive *M. galloprovincialis*.
435 This corresponds to their geographic distribution where *M. trossulus* predominantly inhabit
436 shorelines at higher latitude where winter sub-zero air temperatures are common, while *M.*
437 *galloprovincialis* dominate on warmer low latitude shores (Hilbish et al., 2000). However, the
438 physiological processes behind inter- and intraspecific variation in freeze tolerance remains poorly
439 understood. In *Mytilus* spp., the accumulation of intracellular low molecular weight osmolytes
440 increases freeze tolerance (Kennedy et al., 2020, Williams, 1970), but the accumulation of these
441 putative cryoprotectants can only partly explain survival after sub-zero temperature exposure. For
442 example, although individuals of *M. trossulus* living in the upper intertidal zone are more freeze
443 tolerant than individuals from the low zone, a recent study found no differences in the concentration
444 of metabolites among the shore levels (Kennedy et al., 2020), and no differences in the concentration

445 of cryoprotectants were observed among our three mussel categories, despite large variation in freeze
446 tolerance. Likewise, after ten days of exposure to acidified water that significantly reduced freeze
447 tolerance in all three mussel categories, with the survival of the intertidal population most affected,
448 the low pH exposure had no effect on metabolite concentration in any mussel category, offering no
449 explanation for the observed decrease in freeze tolerance. The fact that the intertidal category was
450 most affected by low pH support our notion that decreased survival was caused by changes in average
451 pH, and not pH variation (see result section 3.4) because animals from more unstable environments
452 (i.e. the intertidal) are generally more resilient to changing environmental conditions (Clark et al.,
453 2018).

454 Another proposed driver of freeze tolerance is the composition of the membrane's phospholipid where
455 a positive relationship between survival and membrane unsaturation state (i.e., higher number of
456 double bonds in the membrane) has been shown in some species (Bindesbøl et al., 2005; Slotsbo et
457 al., 2016). We hypothesized that freeze tolerance in *Mytilus* mussels would also be correlated to
458 unsaturation state, but we observed no significant differences in UI among mussel categories under
459 control pH conditions, and our data show that PUFA and UI in subtidal *M. trossulus* and *M.*
460 *galloprovincialis* decreased in response to OA, yet they were the least affected in terms of freeze
461 tolerance. Meanwhile, intertidal *M. trossulus* had the highest unsaturation stage, but the lowest
462 survival. The phospholipid membrane composition changes have been regarded primarily as an
463 adaptation related to seasonal temperature variability and at our knowledge only one study showed
464 hourly membrane lipids restructuration related to temperature for a cyprinid fish (Carey and Hazel,
465 1989). Our results support that phospholipid composition is of limited importance for freeze tolerance
466 in *Mytilus* mussels, while membrane reconfiguration seems to be important for keeping membranes
467 functional in cold water environments (Pernet et al., 2007; Thyrring et al., 2017c), thus membrane
468 reconfiguration may be important for species to inhabit cold subtidal environments.

While we were unable to explain the variation in freeze tolerance under present-day and acidified conditions, variation in freeze tolerance among populations and congeners may be explained by high molecular weight cryoprotectants, e.g., ice binding proteins, not measured here. Indeed, the influence of antifreeze proteins on freeze tolerance in *Mytilus* ought to be explored further as their potential role seems to vary among populations (Box et al., 2022; Loomis, 1995). Furthermore, thermal tolerance variation may be explained at the gene level (Clark et al., 2021; Peck et al., 2015). A recent study highlighted that differences in the expression of heat shock genes and aquaporins plays a central role in determining freeze tolerance in northern barnacles species (Marshall et al., 2018), and heat shock proteins (HSPs) have been linked to sub-zero temperature survival in insects (Rinehart et al., 2007). Populations from variable environments (such as the intertidal zone or polar regions) are regularly exposed to unpredictable conditions, which can introduce a front-loading of stress genes that enable individuals to better cope with unfavorable conditions. For example, exposure to variable temperatures increases the overall thermal tolerance in the limpet *Lottia digitalis* (Drake et al., 2017), and studies have revealed animals from benign static environments are more vulnerable to unpredictable thermal stress (Marshall et al., 2021; Wang et al., 2020). Front-loading of genes is known from other marine species (Clark et al., 2008; Drake et al., 2017), and freeze tolerant *Mytilus* populations may also have front-loaded genes (e.g. HSPs, aquaporins) that are constantly at a higher expression level, which transfer into resilience through faster production of stress mediating proteins (Barshis et al., 2013). Thus, since the intertidal population of *M. trossulus* are used to daily air exposure, compared to subtidal *M. trossulus* and *M. galloprovincialis*, constantly increased gene expressions may provide an explanation to the difference observed in survival following sub-zero air exposure. Similarly, the subtidal *M. trossulus* mussels were collected in the Burrard Inlet, Vancouver, where the abiotic conditions are variable (Marshall et al., 2021). The exposure to these fluctuating abiotic conditions may also trigger a front-loading of relevant stress genes, and activate the cellular

493 stress response systems (i.e. activating stress proteins such as HSPs (Kültz, 2020)), pre-increasing
494 tolerance to low pH exposure in subtidal *M. trossulus*. *Mytilus galloprovincialis* is known to express
495 the stress regulating gene HSPA12 in response to stressful conditions (You et al., 2013). HSPA12
496 belongs to the HSP70 family, and through a process of gene duplication, HSPA12 acquired subtly
497 different functions, collectively working as a stress regulator (Clark et al., 2021). These stress
498 regulators could, among other things, explain the limited effect of OA on freeze tolerance, and
499 generally the capacity of *M. galloprovincialis* to establish in novel environments. The expression of
500 HSPA12 as a thermal stress mediator was also recently demonstrated in *M. edulis* (Clark et al., 2021),
501 and it is likely that *M. trossulus* also express this protective gene family. Still, intertidal *M. trossulus*
502 may be the most affected by OA because intertidal species generally already live close to their
503 physiological limits and have a limited capacity to adapt to new conditions. The large increase in
504 mortality following low pH exposure may indicate that accommodating this additional environmental
505 stressor exceeds their physiological ability to cope with external stressors. A molecular investigation
506 could reveal the molecular processes behind variation in freeze tolerance among populations and
507 species, and investigations into the underlying genetic mechanisms accounting for our observations
508 would be interesting for future research.
509 Overall, *Mytilus* sp. are excellent at adapting to local environments (Riginos and Cunningham, 2005),
510 making them highly stress tolerant and capable of enduring large ranges of salinities and temperatures
511 (Barrett et al., 2022; Nielsen et al., 2021). Combined with a long pelagic larval period, they have a
512 strong potential to invade new regions (Cárdenas et al., 2020; Thyrring et al., 2017b). This is the first
513 study to investigate the effect of OA on freeze tolerance, an important trait necessary for a poleward
514 shift in the intertidal zone. While intertidal *M. trossulus* populations are found as far north as northern
515 Greenland (Mathiesen et al., 2017), the northern distribution limit of the invasive *M. galloprovincialis*
516 in the Northwest Pacific is set around Canada. At their range edge in the waters of British Columbia,

517 Canada, subtidal populations face intense predation by seastars, excluding mussels from the subtidal
518 and low intertidal (Harley, 2011). The near future pH scenario tested here (pH = 7.5) revealed that
519 acidification weakens freeze tolerance across *Mytilus* spp. (LLT_{50} ~ 7.38 – 7.53°C in intertidal *M.*
520 *trossulus* and *M. galloprovincialis*), and since winter low tides predominantly occurs at nighttime in
521 the Northwest Pacific, occasionally exposing sessile intertidal organisms to air temperatures down to
522 -10°C (Kennedy et al., 2020), significant annual freeze mortality events could occur in both species
523 inhabiting the intertidal if pH continues to decline. Thus, an ongoing poleward expansion in the
524 intertidal (where predation is less intense) could be hindered, offsetting the poleward expanding
525 facilitated by warmer waters. Consequently, if temperatures become too high for survival at a species
526 equatorward edge, the combined effects of predation and limited freeze tolerance could result in a
527 niche squeeze (rather than an expansion), substantially threatening persistence of this species in some
528 regions.
529
530 **Data availability**
531 All data necessary for reproducing this work is freely available from the Borealis dataverse
532 Repository (https://borealisdata.ca; DOI available upon acceptance).
533
534 **Declaration of competing interest**
535 The authors declare that they have no known competing financial interests or personal relationships
536 that could have appeared to influence the work reported in this paper.
537 **Acknowledgements**
538 We would like to acknowledge the technical assistance and expertise of researchers at the Hakai
539 Institute, Quadra Island, British Columbia, who conducted the chemical analysis of our discrete
540 seawater samples, and Vancouver Aquarium and by the City of Vancouver for providing water and

transportation. This research has been supported by a Marie Sklodowska-Curie Individual Fellowship (IF) under contract number 797387, and by the Independent Research Fund Denmark (Danmarks Frie Forskningsfond) (DFF-International Postdoc; case no. 7027-00060B). The funding sources was not involved in designing the study design, in the collection, analysis and interpretation of data, in the writing of the report, or in the decision to submit the article for publication.

References

Barrett NJ, Thyrring J, Harper EM, Sejr MK, Sørensen JG, Peck LS, Clark MS. 2022. Molecular responses to thermal and osmotic stress in Arctic intertidal mussels (*Mytilus edulis)*: The limits of resilience. Genes. 13. 155.

Barshis DJ, Ladner JT, Oliver TA, Seneca FO, Traylor-Knowles N, Palumbi SR. 2013. Genomic basis for coral resilience to climate change. Proceedings of the National Academy of Sciences. 110. 1387-1392.

Baumann H, Wallace RB, Tagliaferri T, Gobler CJ. 2015. Large natural pH, CO_2 and O_2 fluctuations in a temperate tidal salt marsh on diel, seasonal, and interannual time scales. Estuaries and Coasts. 38. 220-231.

Bindesbøl AM, Holmstrup M, Damgaard C, Bayley M. 2005. Stress synergy between environmentally realistic levels of copper and frost in the earthworm *Dendrobaena octaedra*. Environmental Toxicology and Chemstry. 24. 1462-7.

Box ICH, Matthews BJ, Marshall KE. 2022. Molecular evidence of intertidal habitats selecting for repeated ice-binding protein evolution in invertebrates. Journal of Experimental Biology. 225. jeb243409.

Brown NEM, Milazzo M, Rastrick SPS, Hall-Spencer JM, Therriault TW, Harley CDG. 2018. Natural acidification changes the timing and rate of succession, alters community structure, and increases homogeneity in marine biofouling communities. Global Change Biology. 24. e112-e127.

Cappello T, Mauceri A, Corsaro C, Maisano M, Parrino V, Lo Paro G, Messina G, Fasulo S. 2013. Impact of environmental pollution on caged mussels *Mytilus galloprovincialis* using NMR-based metabolomics. Marine Pollution Bulletin. 77. 132-139.

Cárdenas L, Leclerc J-C, Bruning P, Garrido I, Détrée C, Figueroa A, Astorga M, Navarro JM, Johnson LE, Carlton JT, Pardo L. 2020. First mussel settlement observed in Antarctica reveals the potential for future invasions. Scientific Reports. 10. 5552.

581 Carey C, Hazel JR. 1989. Diurnal variation in membrane lipid composition of sonoran desert
582 teleosts. Journal of Experimental Biology. 147. 375-391.
583
584 Clark MS, Geissler P, Waller C, Fraser KPP, Barnes DKA, Peck LS. 2008. Low heat-shock
585 thresholds in wild Antarctic inter-tidal limpets (*Nacella concinna*). Cell stress & chaperones.
586 13. 51-58.
587
588 Clark MS, Peck LS, Thyrring J. 2021. Resilience in Greenland intertidal Mytilus: The hidden stress
589 defense. Science of the Total Environment. 767. 144366.
590
591 Clark MS, Thorne MAS, King M, Hipperson H, Hoffman JI, Peck LS. 2018. Life in the intertidal:
592 Cellular responses, methylation and epigenetics. Functional Ecology. 32. 1982-1994.
593
594 Deere JA, Sinclair BJ, Marshall DJ, Chown SL. 2006. Phenotypic plasticity of thermal tolerances in
595 five oribatid mite species from sub-Antarctic Marion Island. J Insect Physiol. 52. 693-700.
596
597 Drake MJ, Miller NA, Todgham AE. 2017. The role of stochastic thermal environments in
598 modulating the thermal physiology of an intertidal limpet, *Lottia digitalis*. Journal of
599 Experimental Biology. 220. 3072-3083.
600
601 Duarte CM, Rodriguez-Navarro AB, Delgado-Huertas A, Krause-Jensen D. 2020. Dense *Mytilus*
602 beds along freshwater-influenced Greenland shores: Resistance to corrosive waters under
603 high food supply. Estuaries and Coasts. 43. 387-395.
604
605 Evans W, Pocock K, Hare A, Weekes C, Hales B, Jackson J, Gurney-Smith H, Mathis JT, Alin SR,
606 Feely RA. 2019. Marine CO_2 patterns in the Northern Salish Sea. Frontiers in Marine
607 Science. 5.
608
609 Fassbender AJ, Sabine CL, Palevsky HI. 2017. Nonuniform ocean acidification and attenuation of
610 the ocean carbon sink. Geophysical Research Letters. 44. 8404-8413.
611
612 Fossheim M, Primicerio R, Johannesen E, Ingvaldsen RB, Aschan MM, Dolgov AV. 2015. Recent
613 warming leads to a rapid borealization of fish communities in the Arctic. Nature Climate
614 Change. 5. 673-677.
615
616 Franzova VA, MacLeod CD, Wang T, Harley CDG. 2019. Complex and interactive effects of ocean
617 acidification and warming on the life span of a marine trematode parasite. International
618 Journal of Parasitology. 49. 1015-1021.
619
620 Harley CDG. 2011. Climate change, keystone predation, and biodiversity loss. Science. 334. 1124-
621 1127.
622 Harvey BP, Gwynn-Jones D, Moore PJ. 2013. Meta-analysis reveals complex marine biological
623 responses to the interactive effects of ocean acidification and warming. Ecology and
624 evolution. 3. 1016-1030.
625
626 Hazel JR. 1995. Thermal adaptation in biological membranes: Is homeoviscous adaptation the
627 explanation? Annual Review of Physiology. 57. 19-42.

Hilbish TJ, Mullinax A, Dolven SI, Meyer A, Koehn RK, Rawson PD. 2000. Origin of the antitropical distribution pattern in marine mussels (*Mytilus* spp.): routes and timing of transequatorial migration. Marine Biology. 136. 69-77.

Hofmann GE, Smith JE, Johnson KS, Send U, Levin LA, Micheli F, Paytan A, Price NN, Peterson B, Takeshita Y, Matson PG, Crook ED, Kroeker KJ, Gambi MC, Rivest EB, Frieder CA, Yu PC, Martz TR. 2011. High-frequency dynamics of ocean pH: A multi-ecosystem comparison. PLOS ONE. 6. e28983.

Hönisch B, Ridgwell A, Schmidt DN, Thomas E, Gibbs SJ, Sluijs A, Zeebe R, Kump L, Martindale RC, Greene SE, Kiessling W, Ries J, Zachos JC, Royer DL, Barker S, Marchitto TM, Moyer R, Pelejero C, Ziveri P, Foster GL, Williams B. 2012. The geological record of ocean acidification. Science. 335. 1058-1063.

Ianson D, Allen SE, Moore-Maley BL, Johannessen SC, Macdonald, W. R. 2016. Vulnerability of a semienclosed estuarine sea to ocean acidification in contrast with hypoxia. Geophysical Research Letters. 43. 5793-5801.

Jahagirdar S, Saccenti E. 2020. On the use of correlation and MI as a measure of metabolite-metabolite association for network differential connectivity analysis. Metabolites. 10.

Kennedy JR, Harley CDG, Marshall KE. 2020. Drivers of plasticity in freeze tolerance in the intertidal mussel *Mytilus trossulus*. Journal of Experimental Biology. 223.

Kortsch S, Primicerio R, Beuchel F, Renaud PE, Rodrigues J, Lønne OJ, Gulliksen B. 2012. Climate-driven regime shifts in Arctic marine benthos. Proceedings of the National Academy of Sciences. 109. 14052-14057.

Kroeker KJ, Kordas RL, Crim RN, Singh GG. 2010. Meta-analysis reveals negative yet variable effects of ocean acidification on marine organisms. Ecology Letters. 13. 1419-1434.

Kroeker KJ, Sanford E, Rose JM, Blanchette CA, Chan F, Chavez FP, Gaylord B, Helmuth B, Hill TM, Hofmann GE, McManus MA, Menge BA, Nielsen KJ, Raimondi PT, Russell AD, Washburn L. 2016. Interacting environmental mosaics drive geographic variation in mussel performance and predation vulnerability. Ecology Letters. 19. 771-779.

Kültz D. 2020. Evolution of cellular stress response mechanisms. Journal of Experimental Zoology Part A: Ecological and Integrative Physiology. 333. 359-378.

Lim EG, Harley CDG. 2018. Caprellid amphipods (*Caprella* spp.) are vulnerable to both physiological and habitat-mediated effects of ocean acidification. PeerJ. 6. e5327.

Loomis SH. 1995. Freezing tolerance of marine invertebrates. Oceanography and marine biology. 33. 337-350.

Loomis SH, Carpenter JF, Crowe JH. 1988. Identification of strombine and taurine as cryoprotectants in the intertidal bivalve *Mytilus edulis.* Biochimica et Biophysica Acta - Biomembranes. 943. 113-118.

MacLeod CD, Doyle HL, Currie KI. 2015. Technical Note: Maximising accuracy and minimising cost of a potentiometrically regulated ocean acidification simulation system. Biogeosciences. 12. 713-721.

MacLeod CD, Poulin R. 2015. Interactive effects of parasitic infection and ocean acidification on the calcification of a marine gastropod. Marine Ecology Progress Series. 537. 137-150.

Marshall KE, Anderson KM, Brown NEM, Dytnerski JK, Flynn KL, Bernhardt JR, Konecny CA, Gurney-Smith H, Harley CDG. 2021. Whole-organism responses to constant temperatures do not predict responses to variable temperatures in the ecosystem engineer Mytilus trossulus. Proceedings of the Royal Society - Biological sciences. 288. 20202968.

Marshall KE, Dowle EJ, Petrunina A, Kolbasov G, Chan BKK. 2018. Transcriptional dynamics following freezing stress reveal selection for mechanisms of freeze tolerance at the poleward range margin in the cold water intertidal barnacle *Semibalanus balanoides*. bioRxiv. 449330.

Marty Y, Delaunay F, Moal J, Samain JF. 1992. Changes in the fatty acid composition of *Pecten maximus* (L.) during larval development. Journal of Experimental Marine Biology and Ecology. 163. 221-234.

Mathiesen SS, Thyrring J, Hemmer-Hansen J, Berge J, Sukhotin A, Leopold P, Bekaert M, Sejr MK, Nielsen EE. 2017. Genetic diversity and connectivity within *Mytilus* spp. in the subarctic and Arctic. Evolutionary Applications. 10. 39-55.

Menéndez M, Martínez M, Comín FA. 2001. A comparative study of the effect of pH and inorganic carbon resources on the photosynthesis of three floating macroalgae species of a Mediterranean coastal lagoon. Journal of Experimental Marine Biology and Ecology. 256. 123-136.

Meryman HT. 1971. Osmotic stress as a mechanism of freezing injury. Cryobiology. 8. 489-500.

Nagelkerken I, Munday PL. 2016. Animal behaviour shapes the ecological effects of ocean acidification and warming: moving from individual to community-level responses. Global Change Biology. 22. 974-989.

Nielsen MB, Vogensen TK, Thyrring J, Sørensen JG, Sejr MK. 2021. Freshening increases the susceptibility to heat stress in intertidal mussels (Mytilus edulis) from the Arctic. Journal of Animal Ecology. 90. 1515-1524.

Parrish CC. Determination of Total Lipid, Lipid Classes, and Fatty Acids in Aquatic Samples. In: Arts MT, Wainman BC, editors. Lipids in Freshwater Ecosystems. Springer New York, New York, NY, 1999, pp. 4-20.

Peck LS, Thorne MA, Hoffman JI, Morley SA, Clark MS. 2015. Variability among individuals is generated at the gene expression level. Ecology. 96. 2004-14.

723 Pernet F, Tremblay Rj, Comeau L, Guderley H. 2007. Temperature adaptation in two bivalve
724 species from different thermal habitats: energetics and remodelling of membrane lipids.
725 Journal of Experimental Biology. 210. 2999-3014.
726
727 Reid HB, Harley CDG. 2021. Low temperature exposure determines performance and thermal
728 microhabitat use in an intertidal gastropod (*Littorina scutulata*) during the winter. Marine
729 Ecology Progress Series. 660. 105-118.
730
731 Riginos C, Cunningham CW. 2005. Local adaptation and species segregation in two mussel
732 (Mytilus edulis x Mytilus trossulus) hybrid zones. Molecular Ecology. 14. 381-400.
733
734 Rinehart JP, Li A, Yocum GD, Robich RM, Hayward SAL, Denlinger DL. 2007. Up-regulation of
735 heat shock proteins is essential for cold survival during insect diapause. Proceedings of the
736 National Academy of Sciences. 104. 11130-11137.
737
738 Santos IR, Glud RN, Maher D, Erler D, Eyre BD. 2011. Diel coral reef acidification driven by
739 porewater advection in permeable carbonate sands, Heron Island, Great Barrier Reef.
740 Geophysical Research Letters. 38.
741
742 Scrosati R, Eckersley LK. 2007. Thermal insulation of the intertidal zone by the ice foot. Journal of
743 Sea Research. 58. 331-334.
744
745 Sejr MK, Mouritsen KN, Krause-Jensen D, Olesen B, Blicher ME, Thyrring J. 2021. Small scale
746 factors modify impacts of temperature, ice scour and waves and drive rocky intertidal
747 community structure in a Greenland fjord. Frontiers in Marine Science. 7.
748
749 Semesi IS, Beer S, Björk M. 2009. Seagrass photosynthesis controls rates of calcification and
750 photosynthesis of calcareous macroalgae in a tropical seagrass meadow. Marine Ecology
751 Progress Series. 382. 41-47.
752
753 Slotsbo S, Sørensen JG, Holmstrup M, Kostal V, Kellermann V, Overgaard J. 2016. Tropical to
754 subpolar gradient in phospholipid composition suggests adaptive tuning of biological
755 membrane function in drosophilids. Functional Ecology. 30. 759-768.
756
757 Storey KB, Storey JM. 1988. Freeze tolerance in animals. Physiological Reviews. 68. 27-84.
758
759 Storey KB, Storey JM. 1996. Natural freezing survival in animals. Annual Review of Ecology and
760 Systematics. 27. 365-386.
761
762 Sunday JM, Bates AE, Dulvy NK. 2012. Thermal tolerance and the global redistribution of animals.
763 Nature Climate Change. 2. 686-690.
764
765 Telesca L, Peck LS, Sanders T, Thyrring J, Sejr MK, Harper EM. 2019. Biomineralization plasticity
766 and environmental heterogeneity predict geographical resilience patterns of foundation
767 species to future change. Glob Chang Biol. 25. 4179-4193.
768

769 Thyrring J, Blicher ME, Sørensen JG, Wegeberg S, Sejr MK. 2017a. Rising air temperatures will
770 increase intertidal mussel abundance in the Arctic. Marine Ecology Progress Series. 584. 91-
771 104.
772
773 Thyrring J, Jensen KT, Sejr MK. 2017b. Gametogenesis of an intertidal population of *Mytilus*
774 *trossulus* in NW Greenland: not a limitation for potential Arctic range expansion. Marine
775 Ecology Progress Series. 574. 65-74.
776
777 Thyrring J, Juhl BK, Holmstrup M, Blicher ME, Sejr MK. 2015. Does acute lead (Pb)
778 contamination influence membrane fatty acid composition and freeze tolerance in intertidal
779 blue mussels in arctic Greenland? Ecotoxicology. 24. 2036-42.
780
781 Thyrring J, Tremblay R, Sejr MK. 2017c. Importance of ice algae and pelagic phytoplankton as
782 food sources revealed by fatty acid trophic markers in a keystone species (*Mytilus trossulus*)
783 from the High Arctic. Marine Ecology Progress Series. 572. 155-164.
784
785 Thyrring J, Tremblay R, Sejr MK. 2019. Local cold adaption increases the thermal window of
786 temperate mussels in the Arctic. Conservation Physiology. 7. coz098.
787
788 Toxopeus J, Sinclair BJ. 2018. Mechanisms underlying insect freeze tolerance. Biological Reveiws.
789 93. 1891-1914.
790
791 van Heuven S, Pierrot D, Rae J, Lewis E, Wallace DWR. 2011. CO2SYS v 1.1, MATLAB program
792 developed for CO2 system calculations. ORNL/CDIAC-105b. Carbon Dioxide Information
793 Analysis Center, Oak Ridge National Laboratory, U.S. DoE, Oak Ridge, TN.
794
795 Wang J, Peng X, Dong Y. 2020. High abundance and reproductive output of an intertidal limpet
796 (*Siphonaria japonica*) in environments with high thermal predictability. Marine Life
797 Science & Technology. 2. 324-333.
798
799 Wernberg T, Bennett S, Babcock RC, Bettignies Td, Cure K, Depczynski M, Dufois F, Fromont J,
800 Fulton CJ, Hovey RK, Harvey ES, Holmes TH, Kendrick GA, Radford B, Santana-Garcon
801 J, Saunders BJ, Smale DA, Thomsen MS, Tuckett CA, Tuya F, Vanderklift MA, Wilson S.
802 2016. Climate-driven regime shift of a temperate marine ecosystem. Science. 353. 169-172.
803
804 Williams E, Somero G. 1996. Seasonal-, tidal-cycle- and microhabitat-related variation in
805 membrane order of phospholipid vesicles from gills of the intertidal mussel *Mytilus*
806 *californianus*. Journal of Experimental Biology. 199. 1587-96.
807
808 Wishart DS, Feunang YD, Marcu A, Guo AC, Liang K, Vázquez-Fresno R, Sajed T, Johnson D, Li
809 C, Karu N, Sayeeda Z, Lo E, Assempour N, Berjanskii M, Singhal S, Arndt D, Liang Y,
810 Badran H, Grant J, Serra-Cayuela A, Liu Y, Mandal R, Neveu V, Pon A, Knox C, Wilson
811 M, Manach C, Scalbert A. 2018. HMDB 4.0: the human metabolome database for 2018.
812 Nucleic acids research. 46. D608-D617.
813
814 Wittmann AC, Pörtner H-O. 2013. Sensitivities of extant animal taxa to ocean acidification. Nature
815 Climate Change. 3. 995-1001.
816

You L, Ning X, Liu F, Zhao J, Wang Q, Wu H. 2013. The response profiles of HSPA12A and TCTP from *Mytilus galloprovincialis* to pathogen and cadmium challenge. Fish and Shellfish Immunology. 35. 343-50.

Zhao X, Han Y, Chen B, Xia B, Qu K, Liu G. 2020. CO_2-driven ocean acidification weakens mussel shell defense capacity and induces global molecular compensatory responses. Chemosphere. 243. 125415.

Zuur AF, Ieno EN. 2016. A protocol for conducting and presenting results of regression-type analyses. Methods in Ecology and Evolution. 7. 636-645.

Zuur AF, Ieno EN, Elphick CS. 2010. A protocol for data exploration to avoid common statistical problems. Methods in Ecology and Evolution. 1. 3-14.

Figure captions

Figure 1: Proportion survival in intertidal *Mytilus trossulus,* subtidal *M. trossulus* and subtidal *M. galloprovincialis* after subjection to two pH treatments for 10 days and seven sub-zero air temperatures. Lines indicate fitted logistic regression models; Solid black line represent control conditions (pH =7.9) and dashed blue line represent acidified conditions (pH =7.5)**.** Dots represent actual survival and shades areas indicate 95% confidence intervals of the fitted model.

Figure 2: The concentration of common gill tissue osmolytes in intertidal *Mytilus trossulus,* subtidal *M. trossulus* and subtidal *M. galloprovincialis* after subjection to control (pH = 7.9) and acidified (pH = 7.5) conditions (n = 5). The horizontal line in each boxplot is the median, the boxes define the hinges (25–75% quartile) and the whisker is 1.5 times the hinges. Black dots represent data outside this range.

Figure 3: Metabolite-metabolite correlation analysis of gill tissue in intertidal *Mytilus trossulus,* subtidal *M. trossulus* and subtidal *M. galloprovincialis*. Upper panel: metabolite associations after subjection to the control (pH = 7.9) conditions. Lower panel: metabolite associations after subjection

847 to the acidified (pH = 7.5) conditions. Positive correlations are shown in blue; negative correlations
848 are shown in red.

849 **Figure 4:** The molar percentage of saturated fatty acids (SFA), monounsaturated fatty acids (MUFA),
850 polyunsaturated fatty acids (PUFA) of gill tissue in intertidal *Mytilus trossulus,* subtidal *M. trossulus*
851 and subtidal *M. galloprovincialis* after subjection to control (pH = 7.9) and acidified (pH = 7.5)
852 conditions (n = 5). The horizontal line in each boxplot is the median, the boxes define the hinges (25–
853 75% quartile) and the whisker is 1.5 times the hinges. Black dots represent data outside this range.

854

855 **Tables**

856 **Table 1**: Mean (± standard deviation) pH_T and temperature measured directly in aquaria in each
857 incubator.

	Control			Acidified		
Incubator	1	2	3	4	5	6
pH	7.84 ± 0.19	7.92 ± 0.12	7.87 ± 0.13	7.55 ± 0.03	7.49 ± 0.05	7.51 ± 0.06
Temperature	6.67 ± 0.27	6.95 ± 0.36	6.86 ± 0.19	7.17 ± 0.26	7.08 ± 0.54	6.89 ± 0.13

858
859
860
861

862 **Table 2:** Mean percentage (± standard deviation) of 13 fatty acids contributing ~90% of the
863 differences in fatty acid composition after subjection to control (pH = 7.9) and acidified (pH = 7.5)
864 conditions (n = 5). UI = unsaturation index. Bold numbers indicate significant differences among the
865 control and low pH treatment within a mussel category ($p < 0.05$).

	Intertidal - *M. trossulus*		Subtidal - *M. trossulus*		Subtidal - *M. galloprovincialis*	
Fatty acid	Acidified	Control	Acidified	Control	Acidified	Control
16:0	9.53±0.89	8.72±1.21	16.56±6.62	10.21±1.21	12.95±5.17	8.83 ±1.44
18:0	2.57±0.34	2.53±0.17	4.30±1.98	2.28±0.38	3.38±1.26	2.53±0.67
16:1ω7	1.01±0.1	1.2±0.22	**1.58±0.33**	**0.97±0.19**	**1.71±0.33**	**1.07±0.27**
17:1ω7	1.71±0.63	4.07±4.16	1.94±1.14	1.43±1.1	2.26±1.63	2.04±2.15
18.1ω7	1.48±0.12	1.37±0.37	**1.91±0.52**	**1.21±0.2**	2.08±0.58	1.5±0.34
20:1ω9	4.31±0.3	4.12±0.46	**6.21±1.13**	**4.86±0.61**	5.43±1.32	4.37±0.48

18:2ω6	0.91±0.1	0.94±0.35	1.46±0.67	1.31±0.25	0.79±0.36	0.64±0.14
18:3ω3	1.12±0.07	1.21±0.5	1.04±0.57	1.52±0.19	0.31±0.1	0.36±0.09
20.2	9.41±0.76	8.82±1.05	**11.96±1.21**	**9.87±0.58**	9.78±1.79	8.67±1.41
20:4ω6	9.70±1.1	9.81±0.9	3.76±2.61	6.07±0.76	6.95±2.43	9.7±1.37
20:5ω3	9.78±1.15	10.74±1.97	**4.87±3.59**	**12.19±1.05**	7.0±2.98	10.21±1.68
22:2-NMI	11.54±0.84	10.86±1.5	**12.72±0.95**	**9.55±0.66**	13.53±1.5	12.19±.1.14
22:6ω3	14.13±0.99	13.73±0.69	**6.36±4.86**	**16.22±0.48**	**9.7±4.61**	**15.88±2.06**
UI	234.73±6.14	238.84±8.75	**150.94±55.19**	**244.97±4.59**	**187.59±46.35**	**242.92±8.78**

Table 3: Mean (± standard deviation) amino acid composition (% total amino acid content) of gill tissue in intertidal *Mytilus trossulus*, subtidal *M. trossulus* and subtidal *M. galloprovincialis* after subjection to control (pH = 7.9) and acidified (pH = 7.5) conditions (n = 5)

	Intertidal - *M. trossulus*		Subtidal - *M. trossulus*		Subtidal - *M. galloprovincialis*	
Amino acid	Acidified	Control	Acidified	Control	Acidified	Control
Asx	11.18±0.44	11.39±0.25	11.07±0.30	11.34±0.86	11.07±0.30	11.01±0.33
Ala	5.50±0.22	5.74±0.35	5.54±0.21	5.47±0.33	5.54±0.21	5.56±0.13
Arg	7.92±0.85	7.11±0.10	7.07±0.07	7.08±0.11	7.07±0.07	7.22±0.19
Glx	14.08±0.99	14.97±0.16	15.07±0.12	14.81±0.46	15.07±0.12	14.97±0.17
Gly	9.37±0.91	9.15±0.62	9.15±0.61	9.39±1.43	9.15±0.61	9.31±0.7
His	2.03±0.04	2.15±0.12	2.04±0.07	2.09±0.10	2.04±0.07	2.05±0.05
Ile	4.16±0.18	4.14±0.09	4.03±0.16	4.10±0.26	4.03±0.16	3.97±0.19
L-Dopa	0.14±0.01	0.17±0.02	0.09±0.01	0.14±0.03	0.09±0.01	0.11±0.01
Leu	6.49±0.18	6.53±0.09	6.30±0.25	6.42±0.34	6.30±0.25	6.3±0.3
Lys	7.65±1.60	7.06±0.33	6.51±0.37	6.69±1.16	6.51±0.37	6.47±0.36
Met	2.55±0.12	2.60±0.08	2.76±0.05	2.64±0.10	2.76±0.05	2.68±0.08
Phe	4.26±0.19	4.36±0.12	4.16±0.15	4.31±0.44	4.16±0.15	4.08±0.18
Pro	5.25±0.48	5.26±0.27	5.92±0.31	5.59±0.61	5.92±0.31	6.03±0.24
Ser	5.06±0.21	4.85±0.15	4.81±0.10	4.87±0.14	4.81±0.10	4.77±0.1
Thr	4.36±0.16	4.38±0.04	4.72±0.07	4.50±0.13	4.72±0.07	4.75±0.05
Tyr	5.12±0.47	5.25±0.28	5.62±0.10	5.55±0.44	5.62±0.10	5.63±0.15
Val	5.03±0.24	5.06±0.11	5.22±0.10	5.13±0.11	5.22±0.10	5.21±0.08

Abbreviations: Asx, aspartic acid/asparginine; Ala, alanine; Arg, arginine; Glx, glutamic acid/glutamine; Gly, glycine; His, histidine; Ile, isoleucine; Leu, leucine; Lys, lysine; Met, methionine; Phe, phenylalanine; Pro, proline; Ser, serine; Thr, threonine; Tyr, tyrosine; Val, valine.

878

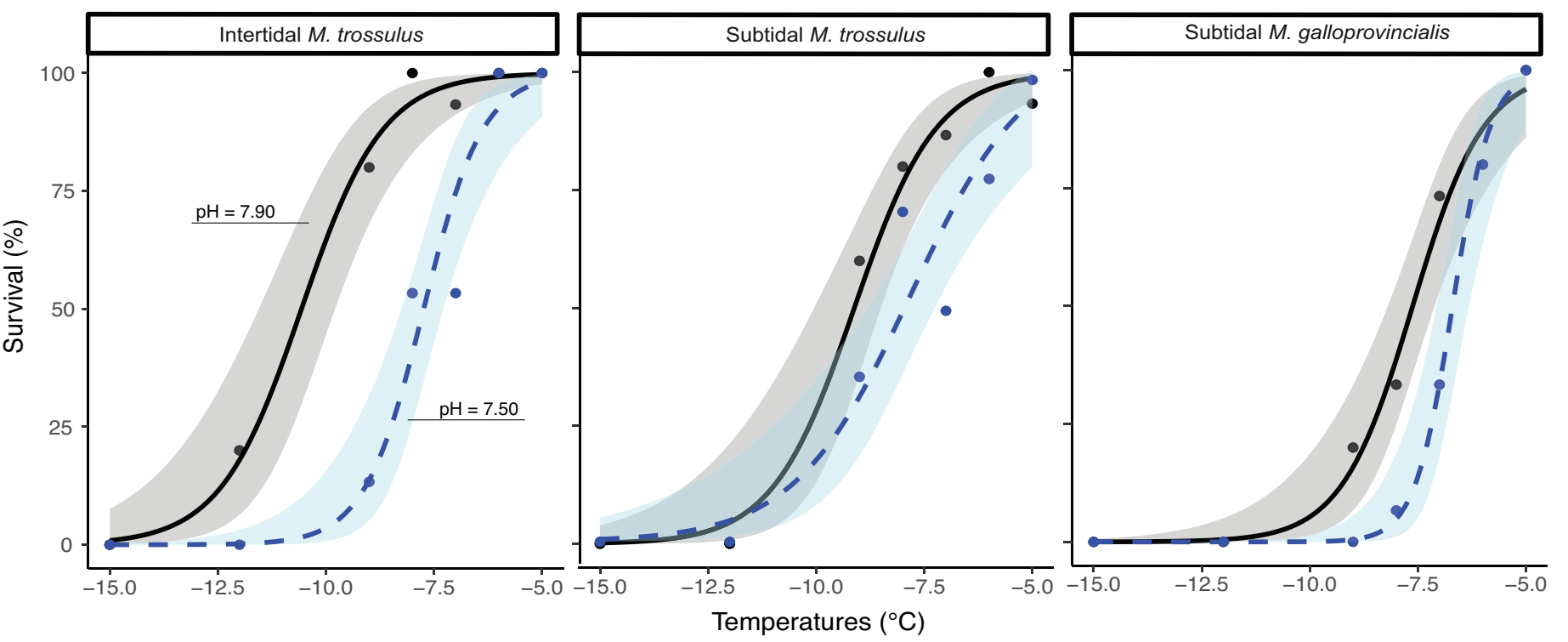
Intertidal M. trossulus
Subtidal M. trossulus
Subtidal M. galloprovincialis
Survival (%)
100
75
50
25
0
pH = 7.90
pH = 7.50
−15.0
−12.5
−10.0
−7.5
−5.0
Temperatures (°C)

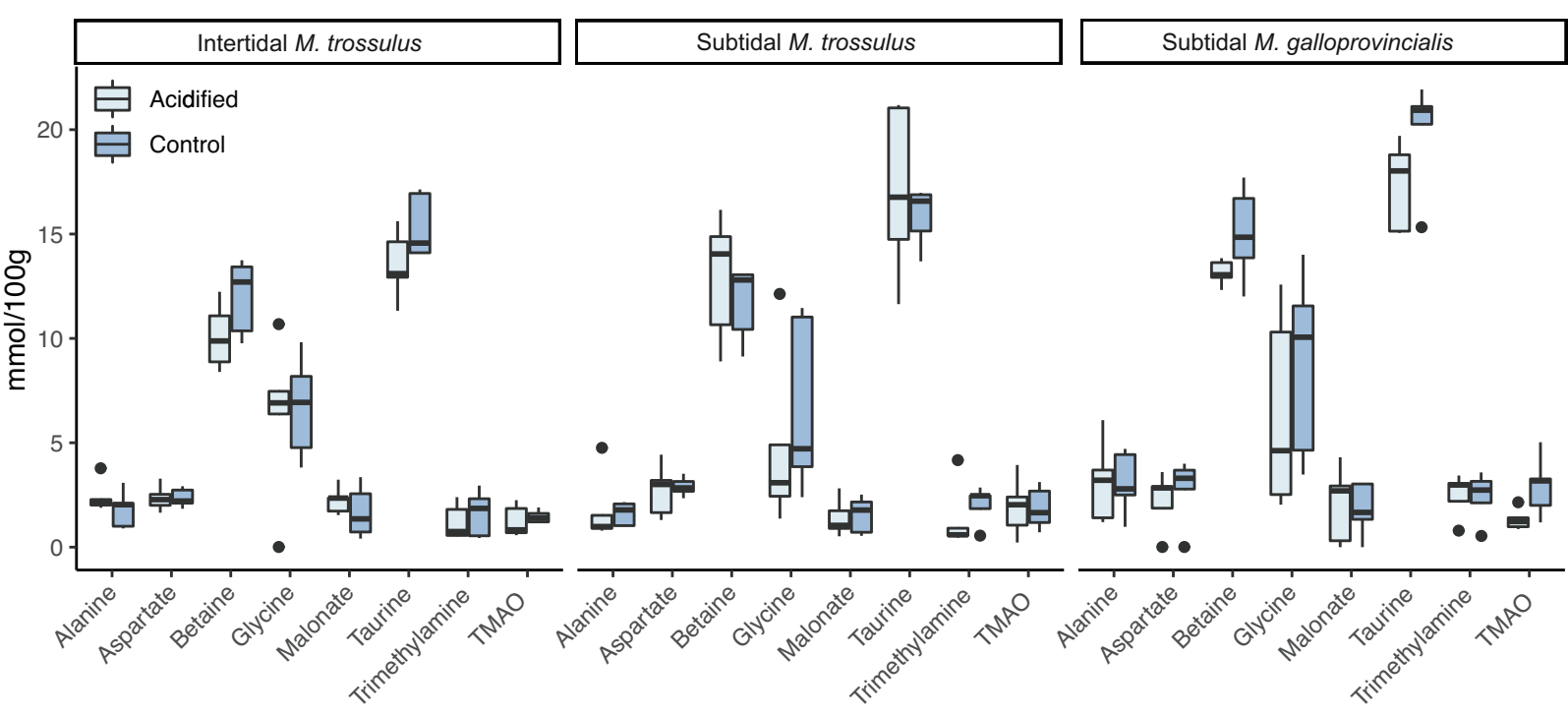
Intertidal M. trossulus
Subtidal M. trossulus
Subtidal M. galloprovincialis
Acidified
Control
mmol/100g
0
5
10
15
20
Alanine
Aspartate
Betaine
Glycine
Malonate
Taurine
Trimethylamine
TMAO

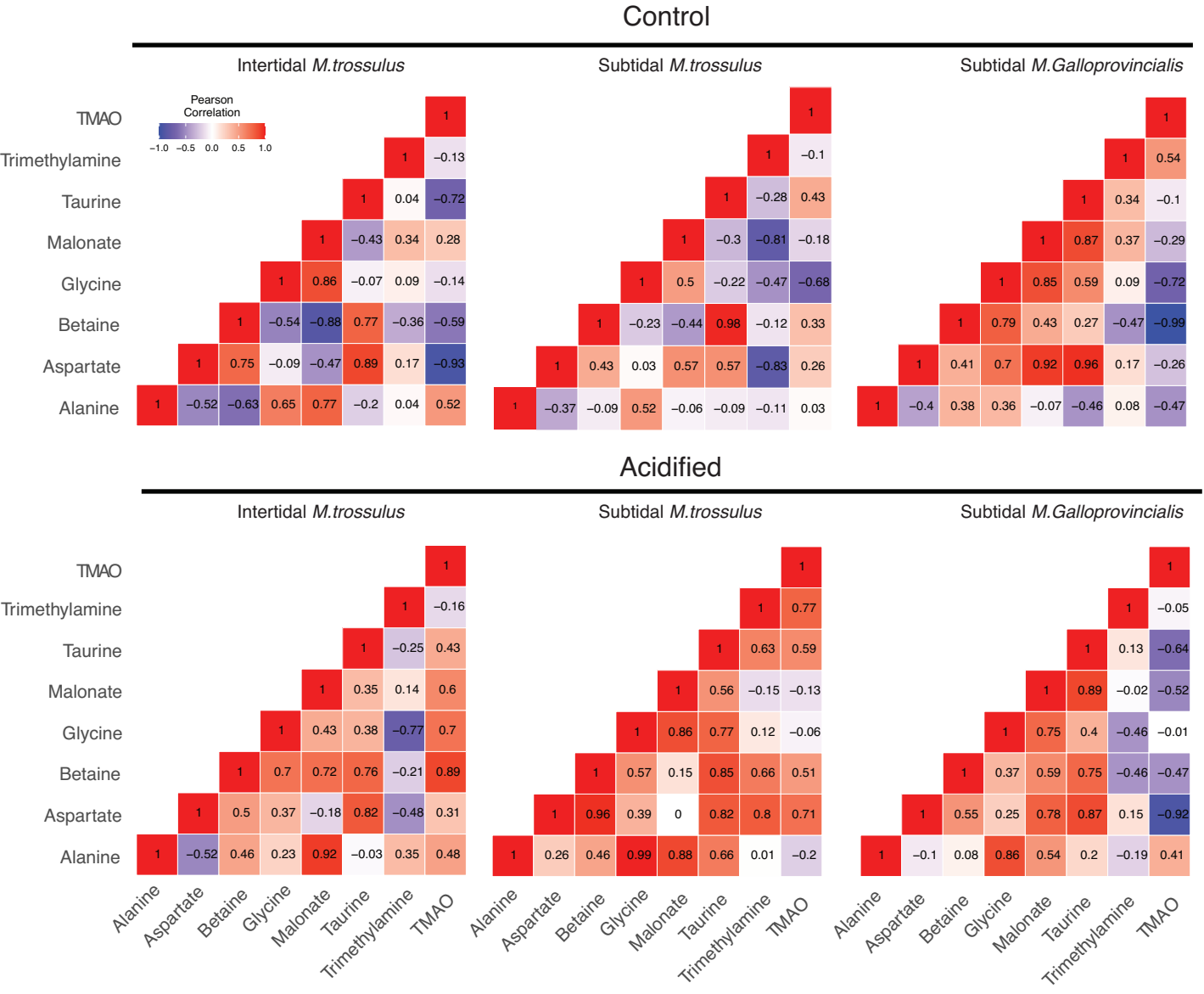
Control
Intertidal M.trossulus
Subtidal M.trossulus
Subtidal M.Galloprovincialis
Pearson Correlation
−1.0 −0.5 0.0 0.5 1.0
TMAO
Trimethylamine
Taurine
Malonate
Glycine
Betaine
Aspartate
Alanine
1
−0.13 1
0.04 −0.72 1
−0.43 0.34 0.28 1
0.86 −0.07 0.09 −0.14 1
−0.54 −0.88 0.77 −0.36 −0.59 1
0.75 −0.09 −0.47 0.89 0.17 −0.93 1
1 −0.52 −0.63 0.65 0.77 −0.2 0.04 0.52
−0.1 1
−0.28 0.43 1
−0.3 −0.81 −0.18 1
0.5 −0.22 −0.47 −0.68 1
−0.23 −0.44 0.98 −0.12 0.33 1
0.43 0.03 0.57 0.57 −0.83 0.26 1
1 −0.37 −0.09 0.52 −0.06 −0.09 −0.11 0.03
0.54 1
0.34 −0.1 1
0.87 0.37 −0.29 1
0.85 0.59 0.09 −0.72 1
0.79 0.43 0.27 −0.47 −0.99 1
0.41 0.7 0.92 0.96 0.17 −0.26 1
1 −0.4 0.38 0.36 −0.07 −0.46 0.08 −0.47
Acidified
Intertidal M.trossulus
Subtidal M.trossulus
Subtidal M.Galloprovincialis
TMAO
Trimethylamine
Taurine
Malonate
Glycine
Betaine
Aspartate
Alanine
1
−0.16 1
−0.25 0.43 1
0.35 0.14 0.6 1
0.43 0.38 −0.77 0.7 1
0.7 0.72 0.76 −0.21 0.89 1
0.5 0.37 −0.18 0.82 −0.48 0.31 1
1 −0.52 0.46 0.23 0.92 −0.03 0.35 0.48
0.77 1
0.63 0.59 1
0.56 −0.15 −0.13 1
0.86 0.77 0.12 −0.06 1
0.57 0.15 0.85 0.66 0.51 1
0.96 0.39 0 0.82 0.8 0.71 1
1 0.26 0.46 0.99 0.88 0.66 0.01 −0.2
−0.05 1
0.13 −0.64 1
0.89 −0.02 −0.52 1
0.75 0.4 −0.46 −0.01 1
0.37 0.59 0.75 −0.46 −0.47 1
0.55 0.25 0.78 0.87 0.15 −0.92 1
1 −0.1 0.08 0.86 0.54 0.2 −0.19 0.41
Alanine
Aspartate
Betaine
Glycine
Malonate
Taurine
Trimethylamine
TMAO

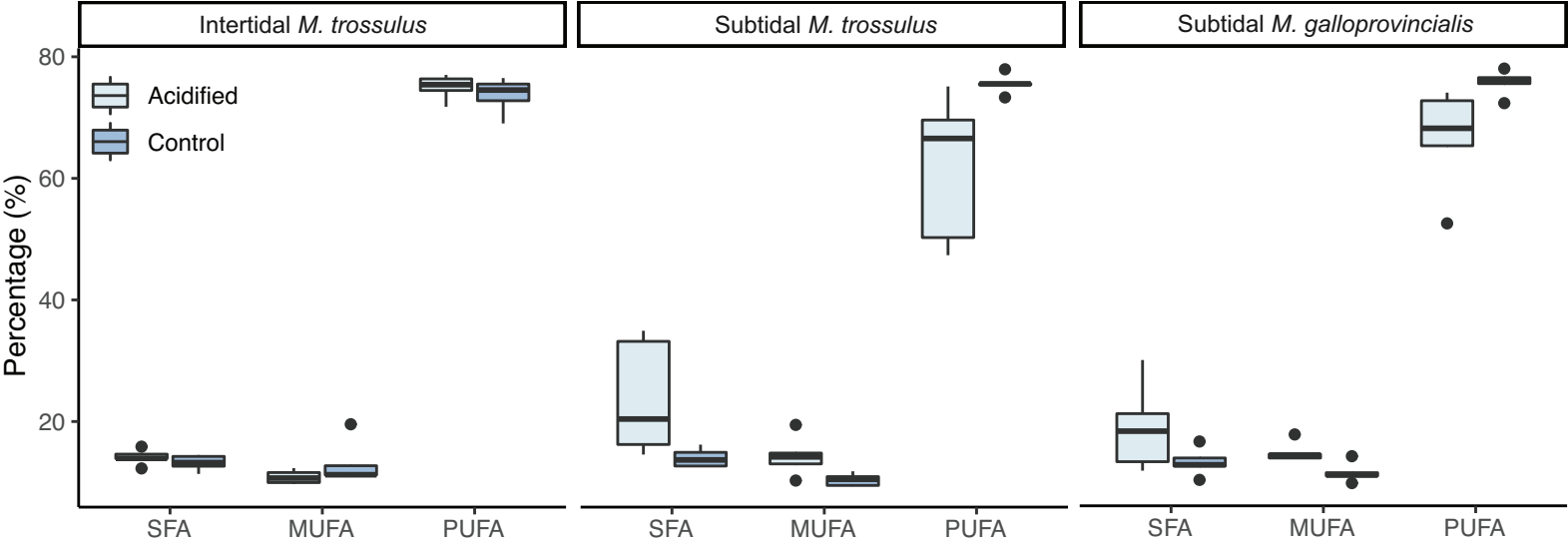
Intertidal M. trossulus
Subtidal M. trossulus
Subtidal M. galloprovincialis
Acidified
Control
Percentage (%)
80
60
40
20
SFA
MUFA
PUFA

Title

Ocean acidification increases susceptibility to sub-zero air temperatures in ecosystem engineers (*Mytilus* sp.): a limit to poleward range shifts

Authors and addresses

Jakob Thyrring[1,2*], Colin D. MacLeod[1,3], Katie E. Marshall[1], Jessica Kennedy[1], Réjean Tremblay[4] & Christopher D. G. Harley[1,5]

[1]Department of Zoology, University of British Columbia, V6T 1Z4, Vancouver, British Columbia, Canada
[2]Department of Ecoscience – Marine Ecology & Arctic Research Centre, Aarhus University, 8600, Silkeborg, Denmark
[3]Department of Biological Sciences, University of Alberta, Edmonton, Alberta T6G 2E9, Canada
[4]Institut des sciences de la mer, Université du Québec à Rimouski, G5L 3A Rimouski, Quebec, Canada
[5]Institute for the Oceans and Fisheries, University of British Columbia, Vancouver, BC V6T 1Z4, Canada

*Corresponding author: thyrring@ecos.au.dk

ORCID
Jakob Thyrring – 0000-0002-1029-3105
Colin MacLeod – 0000-0002-5963-3713
Katie Marshall – 0000-0002-6991-4957
Jessica Kennedy - 0000-0002-7979-1516
Réjean Tremblay – 0000-0003-2590-8915
Christopher D.G. Harley – 0000-0003-4099-943X

Keywords
Blue mussel; Climate Change, Interactions, Intertidal; Fatty acids; $LLT_{50;}$ Multiple stressors; Survival; Thermal tolerance

Figure S1: PCA plot based on (1) ^{1}H NMR identified metabolites and (2) standard amino acids in intertidal *Mytilus trossulus*, subtidal *M. trossulus* and subtidal *M. galloprovincialis* after subjection to control (pH = 7.9) and low (pH = 7.5) pH treatment (n = 5).

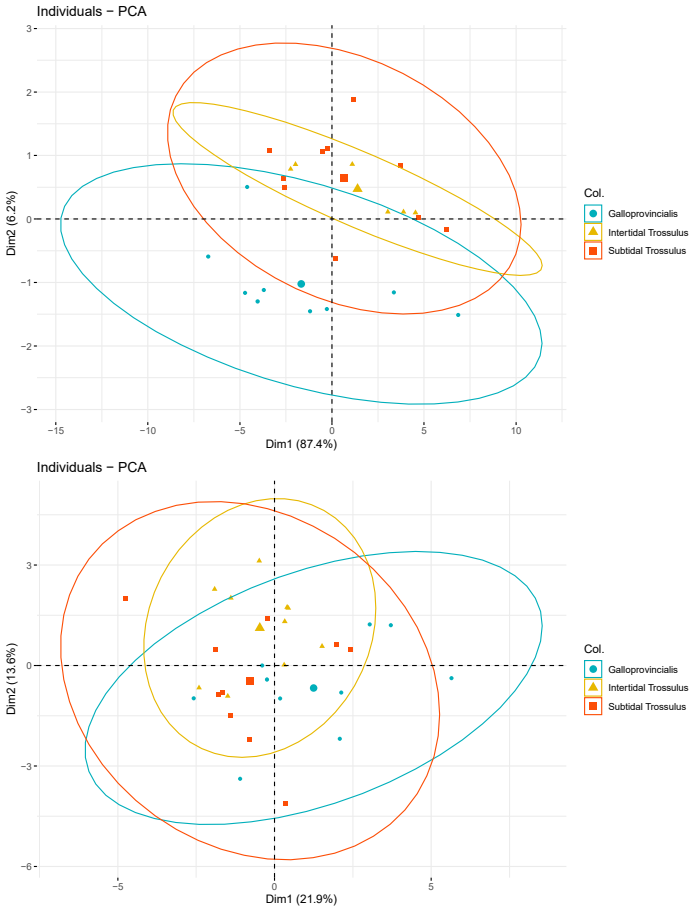

Figure S2: pH measurements from each incubator during the observation period. Incubators 1-3 were set to control conditions (pH = 7.9), while incubators 4-6 were set to acidified conditions (pH = 7.5).

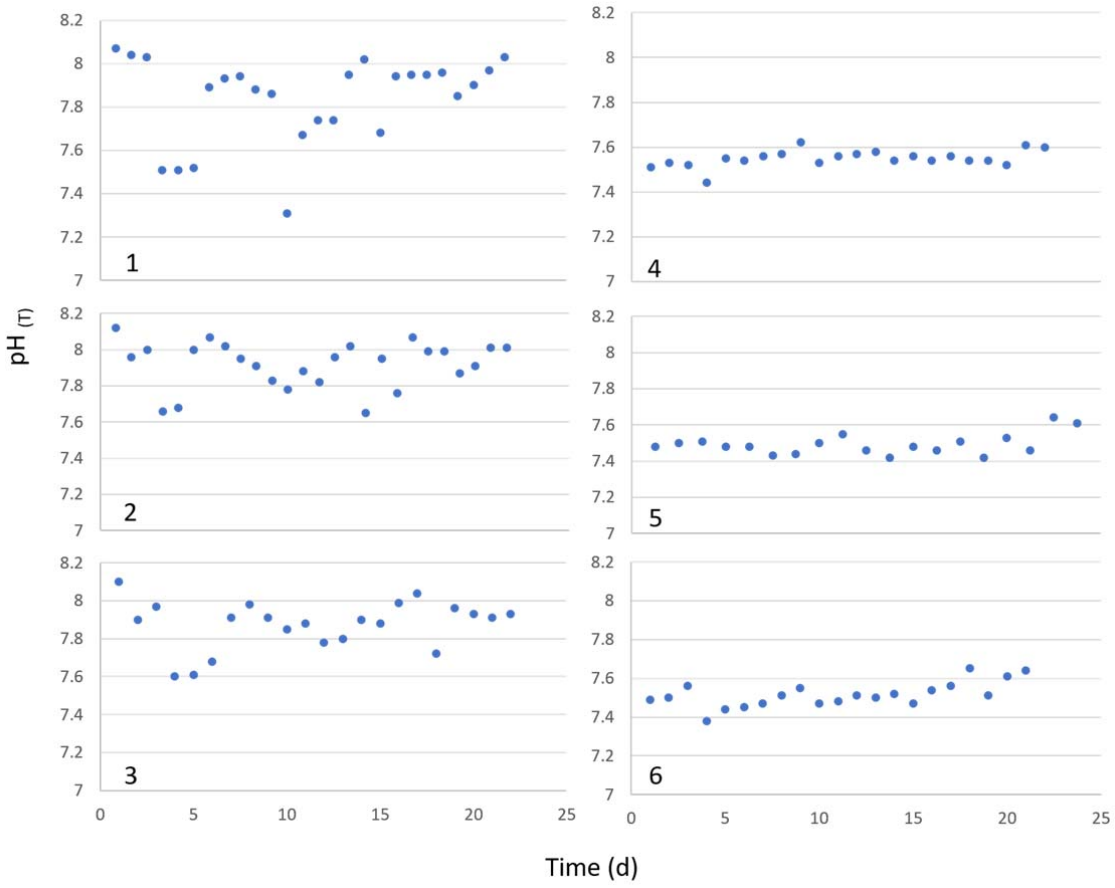

Table S1: Carbonate measurement data from the burke-o-lator system at Hakai Institute. Bold numbers indicate anomalous values.

Treatment	Incubator	DIC (µmol/kg)	TA (µmol/kg)	pCO2 (µatm)	pH (total)	Aragonite (Ω)	Calcite (Ω)
Control (start)	3	1230.64	1335.34	176.67	8.19	1.07	1.76
Control (start)	1	1260.26	1362.46	188.24	8.17	1.06	1.74
Control (start)	2	1272.46	1316.33	361.12	7.90	0.58	0.96
Control (end)	3	**916.80**	**986.24**	**170.48**	8.08	0.63	1.04
Control (end)	2	**705.92**	**776.96**	**115.85**	8.13	0.55	0.90
Control (end)	1	**798.98**	**883.86**	**118.12**	8.17	0.69	1.13
Acidified (start)	5	1421.88	1433.95	621.42	7.71	0.42	0.70
Acidified (start)	6	1516.80	1455.56	1548.91	7.34	0.19	0.31
Acidified (start)	4	1599.63	1607.00	735.82	7.69	0.45	0.75
Acidified (end)	5	1620.13	1637.31	678.28	7.73	0.52	0.85
Acidified (end)	4	1712.32	1653.04	1600.13	7.37	0.24	0.39
Acidified (end)	6	1380.71	1357.44	985.94	7.49	0.26	0.42

Table S2: Mean percentage (± standard deviation) of all fatty acids after subjection to control (pH = 7.9) and acidified (pH = 7.5) conditions (n = 5). The summarized degree of SFA, MUFA and PUFA is presented.

	M. trossulus - intertidal		*M. trossulus* - subtidal		*M. galloprovincialis* - subtidal	
Fatty acid	Acidified	Control	Acidified	Control	Acidified	Control
14:0	0.40±0.07	0.4±0.09	0.54±0.24	0.3±0.05	0.62±0.14	0.37±0.07
15:0	0.52±0.04	0.51±0.05	0.69±0.21	0.41±0.05	0.63±0.26	0.44±0.09
15.0iso	0.07±0.06	0.09±0.1	0.2±0.19	0.16±0.06	0.00	0.08±0.05
16:0	9.53±0.89	8.72±1.21	16.56±6.62	10.21±1.21	12.95±5.17	8.83 ±1.44
17.0	0.45±0.05	0.43±0.04	0.88±0.58	0.38±0.05	0.61±0.28	0.41±0.09
17.0iso	0.3±0.07	0.29±0.05	0.29±0.13	0.12±0.02	0.24±0.07	0.19±0.02
17.0ante	0.17±0.03	0.14±0.02	0.19±0.09	0.08±0.01	0.17±0.06	0.12±0.03
18.0	2.57±0.34	2.53±0.17	4.30±1.98	2.28±0.38	3.38±1.26	2.53±0.67
18.0iso	0.11±0.01	0.1±0.02	0.21±.011	0.08±0.01	0.21±0.07	0.17±0.03
∑SFA	**14.12±1.31**	**13.2±1.27**	**23.86±9.57**	**14.03±1.53**	**18.81±7.26**	**13.12±2.3**
16:1n7	1.01±0.1	1.2±0.22	1.58±0.33	0.97±0.19	1.71±0.33	1.07±0.27
17.1n7	1.71±0.63	4.07±4.16	1.94±1.14	1.43±1.1	2.26±1.63	2.04±2.15
18.1n7	1.48±0.12	1.37±0.37	1.91±0.52	1.21±0.2	2.08±0.58	1.5±0.34
18.1n9	1.04±0.16	1.01±0.24	1.23±0.32	1.07±0.29	1.2±0.33	0.97±0.26
20.1n7	0.65±0.1	0.60±0.14	0.75±0.2	0.34±0.06	0.97±0.27	0.61±0.12
20.1n9	4.31±0.3	4.12±0.46	6.21±1.13	4.86±0.61	5.43±1.32	4.37±0.48
20.1n11	0.67±0.14	0.74±0.19	0.74±0.15	0.53±0.08	1.14±0.19	0.82±0.15
∑MUFA	**10.87±1.1**	**13.13±3.68**	**14.36±3.33**	**10.41±1.02**	**14.78±1.65**	**11.39±1.63**
18.2n6	0.91±0.1	0.94±0.35	1.46±0.67	1.31±0.25	0.79±0.36	0.64±0.14
18.3n3	1.12±0.07	1.21±0.5	1.04±0.57	1.52±0.19	0.31±0.1	0.36±0.09
18.4n3	0.76±0.19	1.07±0.41	0.67±0.25	1.09±0.28	0.39±0.13	0.33±0.11
20.2n6	0.44±0.09	0.46±0.18	0.51±0.22	0.67±0.08	0.32±0.09	0.3±0.04
20.2n	9.41±0.76	8.82±1.05	11.96±1.21	9.87±0.58	9.78±1.79	8.67±1.41
20.3n6	0.11±0.02	0.12±0.04	0.00	0.09±0.02	0.16±0.03	0.12±0.02
20.4n6	9.7±1.1	9.81±0.9	3.76±2.61	6.07√0.76	6.95±2.43	9.7±1.37
20.5n3	9.78±1.15	10.74±1.97	4.87±3.59	12.19±1.05	7.0±2.98	10.21±1.68
22.2NMI	11.54±0.84	10.86±1.5	12.72±0.95	9.55±0.66	13.53±1.5	12.19±.1.14
22.6n3	14.13±0.99	13.73±0.69	6.36±4.86	16.22±0.48	9.7±4.61	15.88±2.06
TMTD	0.14±0.19	0.1±0.1	0.51±0.52	0.09±0.07	0.17±0.12	0.12±0.11
PUFA0	1.19±0.23	0.98±0.1	1.51±0.7	2.36±0.42	0.72√0.07	0.81±0.17
PUFA1	2.62±0.52	2.47±0.25	2.84±1.49	4.06±0.34	1.37±0.42	1.72±0.42
PUFA2	0.93±0.26	0.86±0.23	0.4±0.11	0.38±0.08	0.91±0.33	1.09±0.12
PUFA3	0.68±0.11	0.64±0.07	0.46±0.1	0.52±0.05	0.77±0.18	1.14±0.22
PUFA4	11.54±0.8	10.86±1.5	12.72±0.95	9.55±0.66	13.52±1.5	12.19±1.14
∑PUFA	**75.0±2.05**	**73.67±2.93**	**61.78±12.27**	**75.56±1.65**	**66.4±8.57**	**75.49±2.1**

Table S3: Estimated regression parameters, standard errors, z-values and p-values for the binomial generalized linear models (GLM).

GLM Model (Binomial distribution)	Estimate	s.e	z-value	*p*-value
Subtidal *Mytilus galloprovincialis* (Explained deviance = 95.37%)				
Intercept	11.96	1.81	6.59	< 0.0001
Air temperature	1.58	0.24	6.63	< 0.0001
Low pH	-1.42	0.50	-2.82	< 0.0001
Subtidal *Mytilus trossulus* (Explained deviance = 91.49%)				
Intercept	8.11	1.13	7.20	< 0.0001
Air temperature	0.88	0.13	6.84	< 0.0001
Low pH	-1.31	0.43	-3.05	< 0.0001
Intertidal *Mytilus trossulus* (Explained deviance = 93.94%)				
Intercept	12.71	1.83	6.93	< 0.0001
Air temperature	1.21	0.17	6.79	< 0.0001
Low pH	-3.29	0.70	-4.73	< 0.0001
Survival among mussel categories (Explained deviance = 90.7%)				
Intercept	7.08	0.79	11.15	< 0.0001
Air temperature	0.99	0.10	11.32	< 0.0001
Intertidal *Mytilus trossulus*	1.80	0.34	5.97	< 0.0001
Subtidal *Mytilus trossulus*	1.25	0.32	4.45	< 0.0001

Table S4: Mean (± standard deviation) metabolite concentration (nmol / 100 g ww gill tissue) detected from the H^1NMR analysis after subjection to control (pH = 7.9) and acidified (pH = 7.5) conditions (n = 5).

	M. trossulus - intertidal		*M. trossulus* - subtidal		*M. galloprovincialis* - subtidal	
Metabolites	Acidified	Control	Acidified	Control	Acidified	Control
Acetate	0.41±0.09	0.42±0.16	0.46±0.09	0.36±0.12	0.40±0.16	0.50±0.16
Acetoacetate	0.2±0.13	0.12±0.12	0.05±0.07	0.14±0.15	0.11±0.15	0.20±0.22
Alanine	2.43±0.78	1.82±0.90	1.79±1.68	1.61±0.56	3.12±1.98	3.08±1.53
AMP	0.47±0.47	0.37±0.12	0.54±0.22	0.55±0.45	0.70±0.36	0.56±0.24
Arginine	0.46±1.04	0	0	0	0.36±0.8	0
Asparagine	0	0	0.21±0.48	0	0	0
Aspartate	2.35±0.62	2.36±0.45	2.72±1.26	2.90±0.45	2.24±1.4	2.75±1.60
Betaine	10.09±1.58	12.0±1.82	12.93±3.04	11.70±1.81	13.15±0.61	15.03±2.26
Glutamate	2.52±4.60	0.35±0.53	0.56±0.87	0	0.13±0.28	0
Glycine	6.29±3.90	6.70±2.45	4.79±4.30	6.69±4.24	6.41±4.76	8.75±4.52
Guanidoacetate	0.18±0.29	0.025±0.06	0.16±0.26	0	0.07±0.09	0
Lactate	0.22±0.16	0.38±0.34	0.04±0.06	0.16±0.10	0.47±0.35	0.53±0.24
Lysine	0.15±0.34	0	0	0	0.25±0.56	0.41±0.91
Malate	0.42±0.93	0	1.04±1.44	0	0.36±0.81	0
Malonate	2.24±0.67	1.70±1.25	1.40±0.91	1.54±0.88	2.05±1.84	1.82±1.28
Proline	0.55±0.76	0	0	0.27±0.60	0.67±0.92	0
Succinate	0.31±0.10	0.16±0.11	0.36±0.26	0.35±0.24	0.30±0.24	0.41±0.21
Taurine	13.52±1.66	15.36±1.54	17.07±4.11	15.85±1.42	17.34±2.14	19.91±2.62
Trimethylamine	1.21±0.85	1.62±1.10	1.33±1.59	2.04±0.90	2.49±1.05	2.43±1.19
TAMO	1.24±0.76	1.46±0.30	1.93±1.41	1.87±1.01	1.32±0.50	2.93±1.46
β-Alanine	0.87±0.34	0.68±0.56	0.26±0.43	0.54±0.43	0.55±0.67	0.45±0.35

Table S5: Mean (± standard deviation) carbonate measurements taken from discrete water samples at the start and end of the exposure period.

		PSU	pH	Alkalinity	pCO_2	DIC	Ω aragonite	Ω calcite
Control	Start	22.43 ± 0.06	8.09 ± 0.16	1338.04 ± 23.18	242.01 103.32	1254.45 ± 21.50	0.90 ± 0.28	1.49 ± 0.46
	End	23.23 ± 0.32	8.13 ± 0.05	882.35 ± 104.65	134.82 ± 30.91	807.24 ± 105.68	0.62 ± 0.07	1.03 ± 0.12
Low pH	Start	22.53 ± 0.06	7.58 ± 0.21	1498.84 ± 94.29	968.71 ± 505.71	1412.77 ± 88.94	0.36 ± 0.15	0.59 ± 0.24
	End	23.57 ± 0.23	7.53 ± 0.18	1549.26 ± 166.31	1088.12 ± 469.34	1571.05 ± 171.16	0.34 ± 0.16	0.55 ± 0.26